Available online at www.sciencedirect.com
ScienceDirect
Bioelectrochemistry 70 (2007) 469–480
Bioelectrochemistry
www.elsevier.com/locate/bioelechem

Maxwell displacement current allows to study structural changes of gramicidin A in monolayers at the air–water interface

Pavol Vitovič [a], Martin Weis [b], Pavol Tomčík [b], Július Cirák [b], Tibor Hianik [a,*]

[a] Department of Nuclear Physics and Biophysics, Faculty of Mathematics, Physics and Computer Sciences, Comenius University, 842 48 Bratislava, Slovakia
[b] Department of Physics, Faculty of Electroengineering, Slovak University of Technology, 812 19 Bratislava, Slovakia

Received 26 January 2006; received in revised form 29 May 2006; accepted 15 July 2006
Available online 21 July 2006

Abstract

We applied methods of measurement Maxwell displacement current (MDC) pressure–area isotherms and dipole potential for analysis of the properties of gramicidin A (gA) and mixed gA/DMPC monolayers at an air–water interface. The MDC method allowed us to observe the kinetics of formation of secondary structure of gA in monolayers at an air–water interface. We showed, that secondary structure starts to form at rather low area per molecule at which gA monolayers are in gaseous state. Changes of the MDC during compression can be attributed to the reorientation of dipole moments in a gA double helix at area 7 nm^2/molecule, followed by the formation of intertwined double helix of gA. The properties of gA in mixed monolayers depend on the molar fraction of gA/DMPC. At higher molar fractions of gA (around 0.5) the shape of the changes of dipole moment of mixed monolayer was similar to that for pure gA.

The analysis of excess free energy in a gel (18 °C) and in a liquid-crystalline phase (28 °C) allowed us to show influence of the monolayer structural state on the interaction between gA and the phospholipids. In a gel state and at the gA/DMPC molar ratio below 0.17 the aggregates of gA were formed, while above this molar ratio gA interacts favorably with DMPC. In contrast, for DMPC in a liquid-crystalline state aggregation of gA was observed for all molar fractions studied. The effect of formation ordered structures between gA and DMPC is more pronounced at low temperatures.

Keywords: Gramicidin A; Maxwell displacement currents; Area-pressure isotherms; Surface potential; Lipid monolayers; Aggregation

1. Introduction

Gramicidin A (gA) is bacterial peptide composed of 15 amino acid residues secreted from *Bacilus brevis*. Due to its relatively simple structure it is one of the best studied short peptide and it is often used as a model of integral membrane protein [1,2]. The sequence of gA was for the first time reported by Sarges and Witkop [3] and is as follows: formyl-L-Val[1]-D-Gly-L-Ala-D-Leu-L-Ala-D-Val-L-Val-D-Val-L-Trp-D-Leu-L-Trp-D-Leu-L-Trp-D-Leu-L-Trp[15]-ethanolamine. This structure has specific combination of altering L- and D-hydrophobic residues that is responsible for helical conformation of gA. It is known that gA easily incorporates into the bilayer lipid membrane (BLM). Extensive studies of gA in BLM revealed that in lipid environment this peptide maintains single-stranded $\beta^{6,3}$ conformation [4–6]. In a lipid bilayer two gA monomers are oriented with their N-terminals (formyl end) head-to-head, resulting in the formation of the ion channel that spanning the membrane. According to NMR studies the length of gA in DMPC bilayers is 2.5 nm [7]. Cross sectional area of gA in these bilayers was estimated as 2.5 nm^2 [8]. Inner diameter of such a channel is ~ 0.4 nm [9]. The channel is permeable for monovalent, but not for divalent cations [10]. Computer simulations revealed, that gA channel is surrounded by 16 lipids [11,12]. However, in solution and depending on surrounding solvent as well as in a crystalline form, several different interwined helical dimers were

* Corresponding author. Tel.: +421 2 60295683; fax: +421 2 65426774.
E-mail address: hianik@fmph.uniba.sk (T. Hianik).

1567-5394/$ - see front matter © 2006 Elsevier B.V. All rights reserved.
doi:10.1016/j.bioelechem.2006.07.010

reported. These double helical dimers were found also in vesicles of polyunsaturated lipids as well as in planar bilayer lipid membranes at certain conditions (see Ref. [2] for review). Among various secondary structures the double-strand interwined $\beta^{5,6}$ helix is of special interest. It has similar length (2.6–3.0 nm) like gA channel in $\beta^{6,3}$ conformation, and thus represent structural alternative to dimer model of the gA channel in a membrane.

Due to amphiphilic properties, gA forms stable monolayers at an air–water interface. Detailed analysis of PM-IRRAS spectra at several fixed area per molecules in combination with X-ray reflectivity results showed, that at relatively large molecular areas gA is in disordered secondary structure, however at smaller molecular areas it adopts $\beta^{5,6}$ helical conformation with 30° orientation with respect to the direction perpendicular to a monolayer [13]. Application of PM-IRRAS methods to gA in a lipid monolayers revealed, that gA could be in $\beta^{6,3}$ conformation [14]. However, final conformation of gA depends on gA/phospholipid ratio. The $\beta^{6,3}$ conformation is preferred at low gramicidin content in a lipid bilayer [1].

The properties of mixed gA–phospholipid monolayers are rather complex. It has been found that gA aggregates in the dipalmitoyl phosphatidylcholine (DPPC) monolayers in a gel state at very low concentrations (8×10^{-4} mol%). The aggregation was accompanied by formation of flat subunits with "doughnut" shape (up to ~ 150 nm in diameter). Thermodynamic studies of such a system revealed maximum of miscibility of both DPPC and gA at ~ 28 mol% of gA [15]. In this work it was confirmed, that smallest aggregation unit of gA is hexamer, surrounded by 16 lipid molecules, which was in good agreement with the results obtained by the other authors [16].

Important peculiarity of gA is connected with existence of dipole moment caused by presence of tryptophan residues and their indole dipoles. These dipoles interact with dipoles of polar groups of phospholipids and water molecules at a bilayer-water interface [17,18]. Reorientation of the gA and lipid molecules occurred during compression of monolayers resulted in changes of dipole potential, which can be monitored by means of Kelvin probe [19–21]. It has been shown that presence of gA reduces dipole potential of the lipid monolayer depending on the length of hydrophobic chains of phosphatidylcholines [20].

Another informative contactless method for study the physical properties of monolayers is technique based on measurement Maxwell's displacement currents (MDCs) [21,22]. MDCs are generated during compression of the monolayer. This method is suitable to study reorientation of the molecules in the lipid monolayers. Although MDC technique is relatively widespread, up to now it has not been used for study the reorientation of peptides in lipid monolayers. It is expected that formation of secondary structure of gA in a monolayer should be accompanied by changes of dipole moments of molecules and thus should be monitored by MDC technique.

The aim of this work was the study of physical properties of gA and mixed gA/DMPC monolayers at an air–water interface. We have been interested in study of the formation of secondary structure of gA using MDC technique in combination with measurements of area-pressure isotherms and dipole potential.

2. Experimental

2.1. Chemicals and formation of monolayers

Dimyristoylphosphatidylcholine (DMPC) (M_W=678) was purchased from Avanti Polar Lipids (USA), Gramicidin A (gA) (M_W=2000) was from Sigma (USA). For preparation of monolayers DMPC and gA were dissolved in chloroform at concentration 1 mg/ml and at various molar ratios. As a subphase, deionised water (electrical conductivity less then 1 μS cm^{-1}, ELIX 5, Millipore, USA) was used. DMPC, gA or mixed DMPC/gA monolayers were prepared by spreading of a small amount of solutions (approx. 25 μl) on the water subphase of the Langmuir–Blodgett trough using microsyringe (Hamilton, USA). Each monolayer was allowed to equilibrate for 15 min. This time was sufficient for chloroform evaporation and monolayer stabilization.

Computer-controlled miniature trough model 601 M (NIMA Technology, Coventry, UK) was used for the measurement of surface pressure–area isotherms. The trough was equipped with two simultaneously moveable barriers. The maximum and minimum working area was 86 cm^2 and 14 cm^2, respectively. The surface tension (π) of the monolayer was measured by Wilhelmy method with an accuracy of 1 mN/m. All monolayers were compressed at the constant speed of 5 cm^2/min. The trough was thermostated by a water-circulating bath using a LAUDA E200 thermostat (Koenigshofen, Germany) with an accuracy of 0.05 °C. The experiments were performed mostly at the temperatures 18 °C, and 28 °C, when phospholipid molecules (DMPC) have different conformational mobility. At 18 °C the hydrocarbon chains of DMPC are in *trans* conformation, while at 28 °C they undergo *trans-gauche* transitions.

2.2. Dipole potential

The dipole potential ΔV of the monolayer is difference between the potential of a monolayer and that of clean subphase. The measurement of dipole potential allows to analyze changes in the orientation of the molecular dipoles in the monolayer during compression. Presence of the monolayer between electrodes causes changes of the potential based on the Helmholtz equation:

$$\Delta V = \mu_n/(A.\varepsilon_r.\varepsilon_0) \quad (1)$$

where ε_r and ε_0 are the relative dielectric constant of the air ($\varepsilon_r \approx 1$) and the permittivity of vacuum, respectively, μ_n is the normal component of the dipole moment of the molecule and A is the molecular area. The dipole potential was measured by means of the vibrating plate method [23] using high sensitive electrostatic voltmeter 320C and electrode 3250 (Kelvin probe) (TREK Inc., USA), that allowed measuring dipole potential with an accuracy of 1 mV. The probe was situated in the air approx. 1.5 mm above the surface. Computer controlled equipment allowed to measure dipole potential simultaneously with surface pressure. The surface potential was measured on monolayers formed at NIMA 620 trough (NIMA Technology, Coventry,

UK). The dipole potential was measured in respect to the pure subphase. The later potential was taken as zero.

2.3. Maxwell displacement currents

The Maxwell displacement current (MDC) represents the sum of the contributions coming from changes of the orientations of the molecules (dM_z), changes of the number of the molecules under the upper electrode (dN) (Fig. 1) and changes of the surface potential of the pure subphase ($d\phi$):

$$\frac{dQ}{dt} = I = \frac{N}{d} \cdot \frac{dM_z}{dt} + \frac{M_z}{d} \cdot \frac{dN}{dt} + \frac{\varepsilon_0 . S}{d} \cdot \frac{d\phi}{dt} \quad (2)$$

where d is the distance between electrode 1 and water surface, S is the area of electrode 1 and ε_0 is the dielectric constant of vacuum. Because the surface potential of the pure subphase is constant during the experiment, only first two components participate on the MDC [19]. Apparatus for measurement MDC is based on two parallel electrodes. One was immersed in the water and grounded and the second was placed in the air approx. 1.5 mm above the subphase and electrically shielded. The area of the top electrode was approx. 20 cm^2. Current was measured by sensitive electrometer Keithley 617 (Keithley Instruments, USA). The apparatus was connected with computer and the MDC was recorded simultaneously with surface pressure–area isotherms. The MDC was measured on monolayers formed at NIMA 620 trough. The scheme of measurement of the MDC is shown on Fig. 1 (see Ref. [24] for more details).

The MDC technique is sensitive only to dynamic charge processes, which in this experimental setup are caused by lateral compression of the lipid monolayer. Therefore any time-independent charge (mainly structured water layer and additional substances in subphase) distributed near/at the interface has no effect on the MDC. In comparison with conventional electrical measurements of surface potential (by the Kelvin probe method) MDC technique is of considerable advantage for time-dependent studies of reorientation of the molecules in the monolayer. Dipole moment projection analysis by MDC method is very sensitive for evaluation of molecular orientation (so-called 'order parameter') as well as electric state and/or conformation changes of the molecule. This method can be rather informative for study the phospholipid/protein phase transitions and influence of monolayer composition on the intermolecular interactions. In contrast with surface pressure–area isotherm analysis, MDC measurement is extremely sensitive also in the low surface pressure area, where other methods such are excess area, Gibbs free energy, elastic modulus are much less informative.

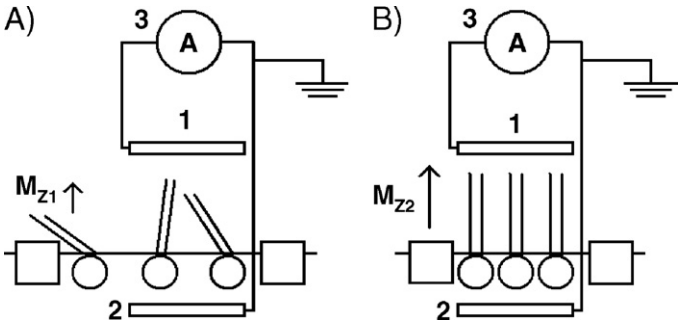

Fig. 1. Scheme of the Maxwell displacement currents (MDC) experimental set-up in the A) gas state and B) solid state of the lipid monolayer. The monolayer is formed between the upper electrode, suspended approx. 1.5 mm above the subphase surface (1) and electrode immersed in the subphase (2). Molecules are forced to change of their orientation, which is accompanied by the flow of the current. Currents induced during compression are detected by sensitive electrometer (3). Change of the orientation of the molecules results in the change of the vertical component of dipole moment (M_{Z1} and M_{Z2} correspond to dipole moments at the gas and solid states, respectively).

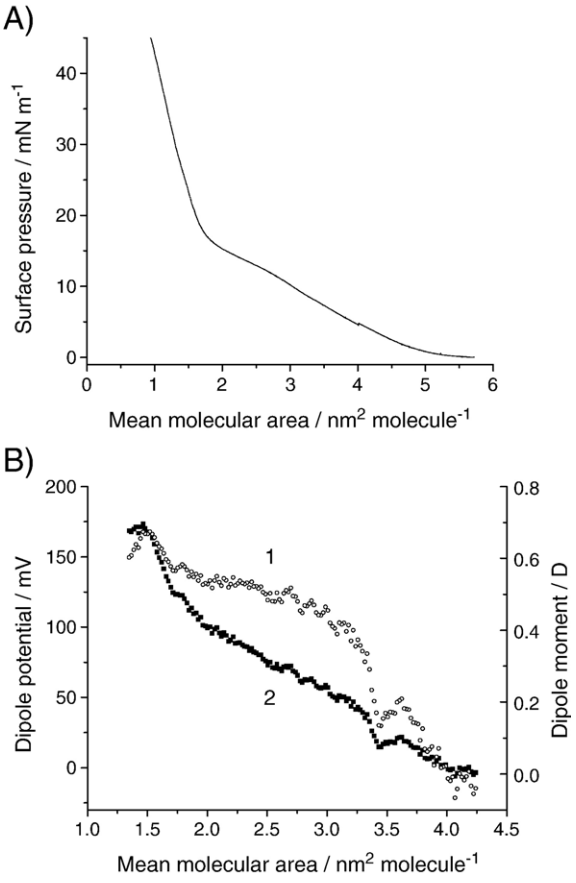

Fig. 2. A) The plot of surface pressure B) dipole potential (curve 1) and dipole moment (curve 2) as a function of mean molecular area for monolayers of pure gA. T=18 °C.

3. Results and discussion

3.1. Gramicidin monolayers at an air–water interface

3.1.1. Pressure–area isotherms

In first series of experiments we studied the properties of the monolayers formed by gA at an air–water interface. We measured the dependence of surface pressure, dipole potential and MDC as a function of area per molecule. As we mentioned in Introduction, gA forms stable monolayers at the water subphase. It is seen on Fig. 2A, where the plot of pressure vs. area per molecule is presented for gA monolayer at T=18 °C.

Pressure–area isotherm has typical shape and is in agreement with previously published results [13,15,25–28]. It is seen that gaseous phase (G) at relatively low pressure at which the area per molecule is >7 nm^2 is transferred to a liquid expanded phase (L-E). Further compression of the monolayer is accompanied by characteristic shoulder with clearly visible plateau at surface pressure $\pi \sim 14$ mN/m. Detailed analysis of the data obtained by PM-IRRAS and X-ray reflectivity studies [13] allowed to connect physical properties of the gA monolayers with changes of secondary structure of gA molecules. The first increase of surface pressure between 0 and 10 mN/m was attributed to formation of interwined β-helix from disordered secondary structure. At the plateau region between 10 and 20 mN/m only density of gA monolayer increases, but molecules are oriented parallel to the monolayer. Sharp increase of surface pressure above 20 mN/m was attributed to tilting of the β-helix. The collapse of the gA monolayer took place at approx. 46 mN/m, which suggest very good monolayer stability. Extrapolation of the part of the isotherm corresponding to the solid state (at surface pressure above 30 mN/m) to the zero surface pressure allows to estimate molecular area per gA molecule, which is approx. 2 nm^2/molecule. This value is in good agreement with the results obtained by the other authors [15,28]. The pressure–area isotherms were recorded also at higher temperature 28 °C and had similar shape and properties like that for 18 °C (results are not shown). It is interesting that similar shape of the area–pressure isotherm was observed also for other short α-helical peptide L_{24} [29]. It is likely, that the transition from disordered to ordered secondary structure for peptides of comparable length took place at similar surface pressures.

3.1.2. Dipole potential of gA monolayers

The plot of dipole potential vs. area per molecule (curve 1) is presented on Fig. 2B. It is seen that dipole potential monotonously increases with decreasing the area per molecule until $A \sim 1.7$ nm^2, when sharper increase of the dipole potential starts. The start of this increase correspond to transition of monolayer into a well ordered film. In this region gA molecules are very close to each other and due to the existence of dipoles of tryptophan at ethanolamine end, the gA molecules interact more strongly. Therefore the final value of the dipole potential reflects not only the changes of the orientation, but also interactions between gA molecules. Using the dipole potential it is possible to estimate dipole moment, μ_n, of gA (see Eq. (1)). In assumption that the relative dielectric constant of the medium (air) is 1, the Eq. (1) can be transformed according to Gaines [30] into the form:

$$\Delta V = 12\pi\mu_n/A \quad (3)$$

where ΔV is dipole potential in mV, A is the area per molecule in $Å^2$/molecule and μ_n is the dipole moment in milliDebye (mD) units. The plot of dipole moment of gA as a function of mean molecular area is shown on Fig. 2B (curve 2). The dipole moment at the area per molecule of 2.5 nm^2, when gA has already well formed secondary structure is around 0.5 D. This value is similar to dipole moment of phospholipids [23]. Small dipole moments at the beginning of compression are due to not established secondary structure of gA as well as due to random orientation of gA molecules. The region of small growth of dipole moment corresponds to the shoulder at π–A isotherm, when gA has already established secondary structure. More detailed information on the kinetics of changes of dipole moment during compression can be obtained by means of MDC method.

3.1.3. MDC of gA monolayers

The plots of MDC as a function of area per molecule for pure gA monolayer during three compression–expansion cycles are presented on Fig. 3. Only curves corresponding to compression are shown for simplicity. The monolayer was compressed only up to surface pressure 35 mN/m at which the molecules are tightly packed, but were still in monolayer form. One can see from Fig. 3 the sharp increase of the current at beginning of the compression that can be connected with the condensation of the gA, formation of ordered secondary structure as well as with certain reorientation of gA molecules during compression. The increase of the number of the molecules under the electrode could also contribute to this effect. Please note that in contrast with the MDC, there is no sharp increase of dipole potential at the beginning of compression (Fig. 2B This is connected with the fact that MDC is more sensitive to reorientation of dipole moments of molecules in comparison with dipole potential measurements. Further increase of the current starting from 6 nm^2/molecule can be connected with increase of the number of molecules under the electrode. The reason of the "hairy" shape of the first compression curve is probably due to not well-ordered monolayer. Subsequent expansion, followed by compressions, resulted better ordering of gA monolayers. Both curves corresponding to the second and the third compressions have higher and more narrow peak at the region ~7.2 nm^2/molecule. This is probably due to better-oriented molecules, and hence better distribution of gA, under the electrode, comparing to the first compression. On the other side, increase of the current at the lower molecular areas is not so dramatic in comparison with first compression, but slowly increases up to ~ 4 nm^2/

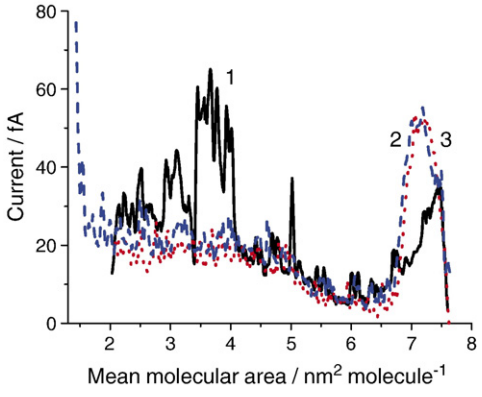

Fig. 3. Maxwell displacement current versus mean molecular area for pure gA monolayer for three subsequent compressions up to 30 mN/m. The number of compression is shown at corresponding curve. T=18 °C.

molecule, when the current reaches steady state value of approx. 20×10^{-15} A (i.e. 20 fA). The MDC is rather low. However, the background current for a pure water subphase without monolayer is around 1–3 fA, i.e. more then one order of magnitude lower in comparison with those for monolayer. Detailed analysis performed earlier [24] showed, that generation of the MDC is not connected with such phenomena as motion of intrinsic ions or ionization of the monolayer and is attributed to reorientation of dipole moments of the molecules from which the monolayer is composed.

More detailed insight into the current–area relation can be seen in Fig. 4 where both surface pressure and current are plotted as a function of area for the third compression–expansion cycle. The stability of the monolayer and the process of the reversibility are proved by almost the same shape of the isotherms corresponding to both compression and expansion. The same holds for the behavior of the MDC, while the shape of the current–area curve at the expansion is the mirror picture of the curve at the compression.

The current starts to grow immediately from the beginning of the compression, although the surface pressure is still zero. As it was already mentioned above, current–area plot can be divided on two parts — first one at the higher areas comes from the formation of ordered secondary structure and possible changes of orientation of the gA molecules as well as due to increased number of the molecules under the electrode. Second one at the lower areas is due to change of the number of the molecules under the electrode. It is likely, that biphasic changes of the current at the beginning of the compression could be connected with formation of secondary structure of gA, namely interwined $\beta^{5,6}$ helix. The current starts to be constant at ~ 4 nm^2/molecule, at the area that is characterized by the appearing the plateau on the isotherm. We should, however note, that exact type of secondary structure can be determined by spectroscopic, but not by MDC method. According to Ref. [13], at this region the secondary structure of gA is already established and the molecules are uniformly ordered in parallel to a monolayer. The sharp increase of the current after 2 nm^2/molecule can be connected with changes of orientation of gA. This is in good agreement

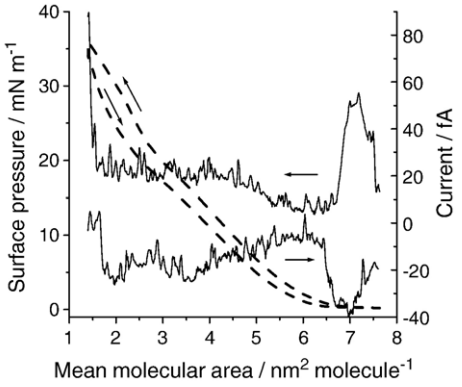

Fig. 4. Surface pressure (dashed line) and Maxwell displacement current (full line) versus mean molecular area of pure gA monolayers for compression and expansion cycles. The direction of compression and expansion is shown by arrows. T=18 °C.

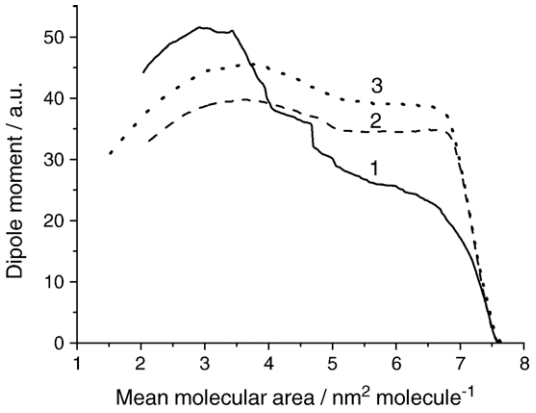

Fig. 5. Dipole moment versus mean molecular area for gA monolayer for three subsequent compressions calculated from MDC presented on Fig. 3. The number of compression is shown at corresponding curve. T=18 °C.

with the results obtained by PM-IRRAS and X-ray reflectivity studies [13].

3.1.4. Dipole moment of gA

The obtained values of MDC allowing to estimate dipole moment of gA molecules. The vertical component of the molecular electric dipole moment is proportional to the changes in the induced charge on the electrode 1 (Fig. 1) and can be expressed as follows:

$$M_z = \frac{G}{N}\int_0^t I(t)\mathrm{d}t \tag{4}$$

where G is geometric factor (in ideal case it is equal to distance from electrode 1 to the subphase [24]) and N is the number of the molecules under the electrode 1 (see Fig. 1). Generally, geometric factor has complicated form and depends on the shape of the electrode, distribution of the charges, shielding etc. Therefore, determination of the dipole moment requires exact knowledge on the geometric factor. In order to avoid problems with geometric factor we expressed the values of dipole moments in arbitrary units (a.u.).

Fig. 5 shows the plot of dipole moment vs. area for gA monolayer calculated using the data presented on Fig. 3. We can see that the curve 1 corresponding to first compression is rather different from that corresponding to second and third compressions. The shape of the curve 1 reflects complicated process of the formation of the monolayer. After the preparation of the monolayer the molecules are randomly distributed and the transitions from one structural state to another do not occur at one moment, but in small steps. These steps are well resolved at areas 5 and 4.7 nm^2/molecule. The dipole moment reaches maximum at the area of 3 nm^2/molecule. The shape of the curves of the subsequent compressions is different from that corresponding to the first compression. It can be expected that after first compression–expansion cycle certain part of the molecules is not oriented parallel to the surface but molecules are tilted under some angle from the position normal to the surface. It is also possible, that molecules form small aggregates that are stable

after compression. On the other side, because at finishing of the first compression (not exceeding the collapse pressure) well ordered monolayer is formed, consecutive expansion spreading the molecules more uniformly, i.e. they are in similar distance from each other. Therefore, further compressions are characterized by more continuous increase of the number of molecules under the electrode, as well as more uniform uprising of the molecules. Better stability of the monolayer can be seen from the shape of the curves corresponding to the second and the third compression. The reorientation of the molecules is more fluent.

From comparison of the plot of both the surface pressure and dipole moment versus mean molecular area of gA monolayer (Figs. 4 and 5) it can be see, that the dipole moment increases with decreasing of mean molecular area until ~ 7 nm^2/molecule when the surface pressure starts to increase. The dipole moment projection remains constant between 5.2 and 7 nm^2/molecule when the monolayer is in the liquid expanded (L-E) state. In line with above discussion it is likely that ordered secondary structure of gA is formed at the mean molecular area of 7 nm^2/molecule. At the region 5.2–7 nm^2/molecule the interwined $\beta^{5,6}$ helix is already established and compression of the monolayer resulted only in more tightly packed molecules, but does not change of gA secondary structure. Phase transition from L-E to liquid-condensed (L-C) state caused further increase of the molecule packing, however increase of dipole moment in this region revealed only changes in gA orientation. The dipole moment reaches maximum at the same area 3.6 nm^2/molecule, where the inflexed point of the plateau is situated. Next phase transition from L-C to solid (S) phase caused dramatic decrease of the dipole moment. We assume that this decrease is not caused by the collapse of the monolayer (monolayer was compressed up to 30 mN/m, i.e. far below from the critical pressure ~ 45 mN/m), but by another reorientation of the molecule.

3.2. Mixed gA/DMPC monolayers at an air–water interface

3.2.1. Pressure–area isotherms

In this section the results of the study of physical properties of mixed gA/phospholipid monolayers are presented. We have been interested how conformational state of the molecules of the monolayer (corresponding to gel or liquid-crystalline state) will affect interaction between gA and phospholipids. As a phospholipid we used dimyristoylphosphatidylcholine (DMPC). Since DMPC has the main phase transition at $T_F \cong 23$ °C, experiments were performed well below (18 °C) and above (28 °C) T_F when the molecules in the monolayer are in a gel or liquid-crystalline state, respectively.

Pressure–area isotherms for pure DMPC, gA and for mixed gA/DMPC monolayers at temperatures 18 and 28 °C are presented on Fig. 6 A and B, respectively (isotherms only for selected molar fractions of gA/DMPC are presented for simplicity, however larger variations of molar fraction was studied and then used in analysis, see below). Isotherms for pure DMPC monolayers have typical shape [31,32] and several regions corresponding to the different structural states of the monolayer can be distinguished. Monolayer is in the liquid-expanded state (L-E) at the high areas per molecule ($A > 0.78$ nm^2) and at the

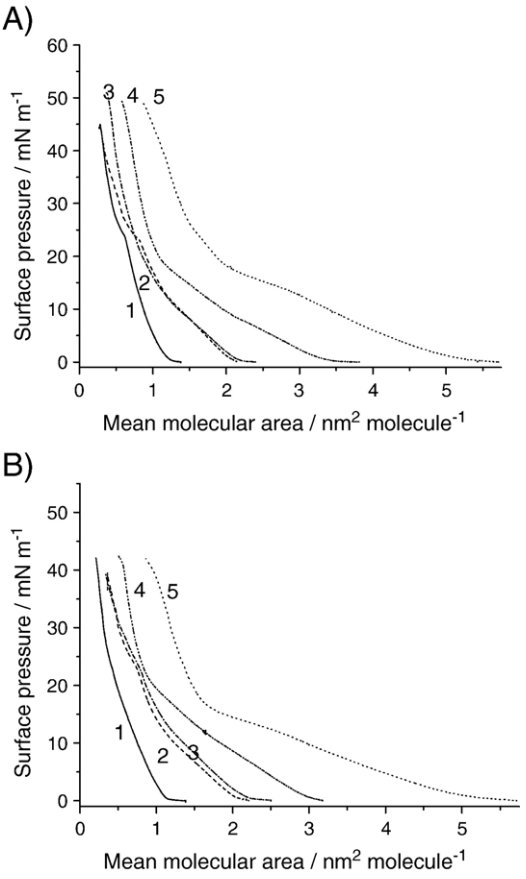

Fig. 6. Pressure–area compression isotherms of gA/DMPC mixed monolayers and pure components at an air–water interface. Curves correspond to various molar fraction of gA. (1) 0 (pure DMPC); (2) 0.17 (3) 0.25 (4) 0.5 (5) 1 (pure gA). The isotherms were recorded at A) 18 °C and B) 28 °C.

surface pressure $\pi \sim 8$ mN/m turns into the liquid-condensed (L-C) state, which is characterized by steeper growth of the surface pressure. Detailed analysis revealed that in a gel state a plateau is observed at the surface pressure $\pi \sim 25$ mN/m (Fig. 6A) that corresponds to the phase transition from L-C to solid (S) state. Molecules in the S state are well oriented and densely packed. Further compression causes lost of two-dimensional form and monolayer collapses at $\pi \sim 45$ mN/m. The mean area per DMPC molecule at S state can be estimated by extrapolation of this part of the isotherm to the zero surface potential: ~ 0.7 nm^2, which is in good agreement with the results obtained by other authors [20]. The phase transition into a liquid-crystalline state is accompanied by lost of the plateau typical for transition from L-C to S state (Fig. 6 B). At the same time, area per molecule in L-C state slightly increases with increasing temperature. Shape of the isotherms of mixed gA/DMPC monolayers depends on the molar fraction of gA in the monolayer. With increasing concentration of gA, the increase of mean molecular area took place.

The analysis of miscibility of both components — gA and DMPC can provide better insight into the mechanisms of DMPC–gA interactions. The value of mean molecular area A_{12} as a function of molar fraction, X=[gA]/([gA]+[DMPC]) ([gA] and [DMPC] are molar concentrations of gA and DMPC,

respectively), of pure components, i.e. gA and DMPC (A_1 and A_2, respectively) can be expressed as follows [32]:

$$A_{12} = X.\mathrm{A}_1 + (1-X).\mathrm{A}_2 \quad (5)$$

In the case of ideal miscibility, the plot of A_{12} vs. X should be straight line connecting the values of mean molecular areas of pure components. Negative deviation from ideal miscibility indicates interaction between molecules, e.g. formation of gA/DMPC complexes, while positive deviation can be related to formation of aggregates of pure components [32]. In order to analyze the properties of gA in a monolayers we constructed the plot of the mean molecular area at surface pressure 35 mN/m as a function of molar concentration of gA. The surface pressure was selected in order to approach properties of the monolayers to that of the lipid bilayers [33]. Fig. 7 shows plot of the mean molecular area vs. molar fraction of gA for DMPC monolayers in a gel (A) and liquid-crystalline state (B), respectively. We can see that these plots are different. In a gel state there is positive deviation from linearity in a range of 0–0.2 molar fraction of gA, while above 0.2 molar fraction of gA the deviation is negative. For a liquid-crystalline state the most remarkable deviation from linearity is in similar range of molar fraction of gA, i.e. 0–0.2, however the deviation remains positive also at higher content of gA. Further insight on the interaction of gA with lipids can be obtained by analysis of the excess free energy, ΔG [32]:

$$\Delta G = \int_0^{\pi} A_{12}\mathrm{d}\pi - X\int_0^{\pi} A_1\mathrm{d}\pi - (1-\mathrm{X})\int_0^{\pi} A_2\mathrm{d}\pi \quad (6)$$

where X is the molar fraction of gA, A_1 and A_2 are mean molecular areas of gA and DMPC, respectively. The lower limit of integration corresponds to $\pi=0$, while upper limit can be arbitrary selected (we selected $\pi=35$ mN/m). The value of ΔG provides information whether the particular interaction is energetically favorable ($\Delta G<0$) or not ($\Delta G>0$), while for $\Delta G=0$ ideal mixing takes place. We therefore calculated the excess free energy for mixed monolayers in a gel and in a liquid-crystalline state. The plot of ΔG as a function of molar fraction of gA in a monolayer is presented in Fig. 8 for monolayers in a gel (A) and in a liquid-crystalline state (B). From Fig. 8A it is seen, that for monolayers in a gel state the value $\Delta G>0$ at the range of 0–0.2 molar fraction of gA, but it is negative above 0.2 molar fraction with inflection point at 0.2 molar fraction. The excess free energy for mixed monolayer in a liquid-crystalline state is positive for all molar fractions of gA. Thus, presented results for monolayers in a gel state and in a range 0–0.2 molar fraction of gA suggests that interaction between gA and lipids is not favorable in this range. This is in agreement with results presented on Fig. 7A and can be explained as the aggregation of gA molecules. The negative value of excess free energy above $X=0.2$ molar fraction of gA suggests that at this range the gA favorable interacts with the lipids and that gA/DMPC complexes exists in this range. It is interesting to compare the results obtained with that published by Diociaiuti et al. [15]. In this paper the authors investigated the properties of gA in a lipid monolayers composed of dipalmitoylphosphatydilcholine (DPPC) in a gel state of monolayers at $T=25$ °C (the temperature of phase transition of DPPC is approx. 41 °C). They also observed the deviation of experimental points from additive rule at gA concentration below 0.2 molar fraction while at 0.3 molar fraction negative deviation from additivity took place. Above this concentration again positive deviation from additive rule was typical for this system. The obtained results were in agreement with calculation of excess free energy. At lower molar fraction of gA (0–0.2) and at a gel state of DMPC monolayers our results agree with that obtained in the mentioned paper, however at higher gA concentration we did not observe positive deviation from linearity. One of the possible reason of these differences consists presumably in different mismatch between gA/DMPC and gA/DPPC due to different length of hydrophobic chains of these two phospholipids. The hydrophobic length of DMPC and DPPC molecules in a gel state of the lipid bilayers is 1.71 and 1.97 nm, respectively [34]. If we assume that the length of hydrocarbon chains of DMPC in a monolayer is similar to that in a bilayer and that in condensed state of the monolayer the gA axis is oriented perpendicular to the monolayer as well as that the length of gA monomer is according to Ketchem et al. [7], 1.25 nm then we can see that the mismatch between gA and lipids is less expressed for DMPC in a gel state. In a liquid

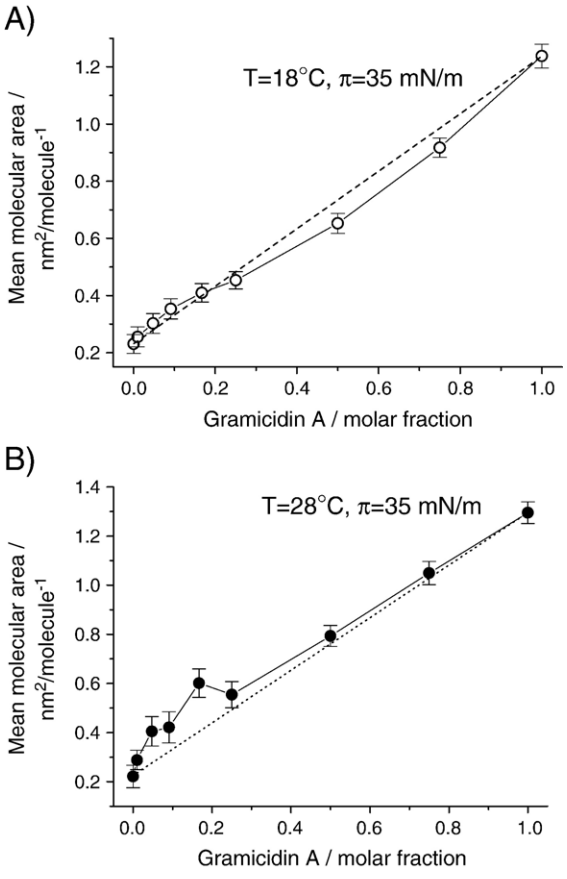

Fig. 7. The plot of mean molecular area versus molar fraction of gA in the gA/DMPC monolayers in a gel state (A) ($T=18$ °C), and in a liquid-crystalline state (B) ($T=28$ °C). The results are mean±SD obtained from 5 independent experiments for each molar content of gA.

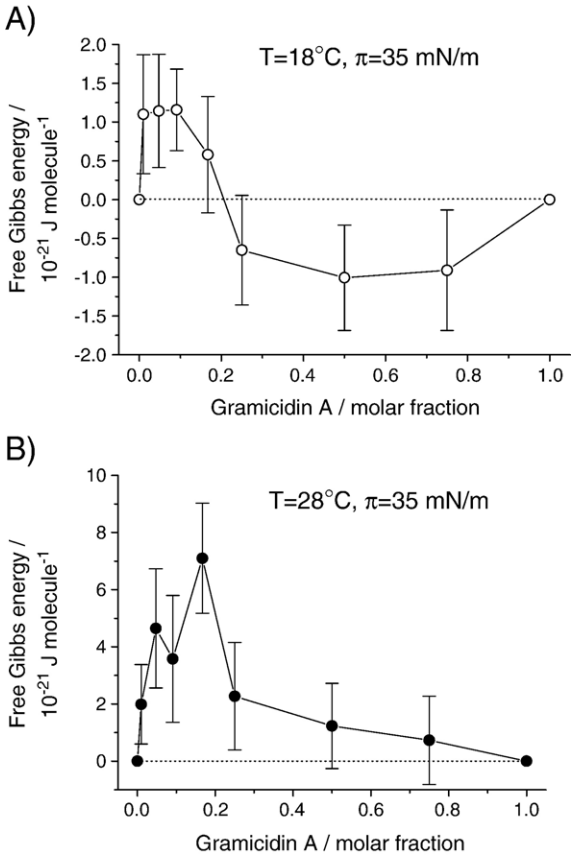

Fig. 8. The plot of excess free energy, ΔG, versus molar fraction of gA in the gA/DMPC monolayers in a gel state (A) (T=18 °C), and in a liquid-crystalline state (B) (T=28 °C). The results are mean±SD obtained from 5 independent experiments for each molar content of gA.

crystalline state the hydrophobic length of DMPC and DPPC is 1.14 and 1.31 nm, respectively [34]. Therefore the mismatch is more expressed for DMPC, while for DPPC there is good fit between hydrophobic length of both lipid and gA monomer. Thus, for DMPC in a liquid-crystalline state the aggregation should be more favorable and it is in fact confirmed by obtained data. On the other hand results obtained in a gel state, especially at higher molar fraction of gA cannot be explained exclusively by mismatch. As it is seen from Figs. 7A and 8A, at the molar fraction above 0.2 the gA favorably interacts with DMPC despite of existing mismatch. It should also be note, that phase transition of phospholipid does not affect the secondary structure of gA [35].

In order to obtain more insights on the properties of gA in lipid monolayers in a gel state we performed experiments focused on measurement of the surface potential and MDC at certain gA/DMPC molar ratios.

3.2.2. Dipole potential of DMPC and mixed gA/DMPC monolayers

The dipole potential–area (*V–A)* and pressure–area (*π–A*) plots for pure DMPC and for mixed gA/DMPC monolayer for molar fraction of 0.25 are presented on Fig. 9 A and B, respectively. For *V–A* curve corresponding to pure DMPC one can see that the increase of the dipole potential starts at the high mean molecular area (~ 1.25 nm^2), when the monolayer is in L-E state. The molecules start to orient themselves and normal component of the dipole moment increases (curve 1, Fig. 9 A). The abrupt stop of the potential increase occurs at ~ 1.1 nm^2, when the surface pressure starts to grow (curve 2, Fig. 9A) and remains practically constant until mean molecular area 0.8 nm^2. We can conclude that in this state the molecules are just getting closer each to another and their tilt angle is constant. Therefore there is no increase of the dipole potential. Another increase of the surface potential can be observed at mean molecular area of ~ 0.75 nm^2. Some structural reorganization of the monolayer occurs that cause not only transition from L-E to L-C state, but also change of the orientation of the molecules. Transition from L-C to S state is characterized by another raise of the dipole potential. The molecules are tightly packed and dipole–dipole interactions can contribute to the final dipole potential. The value of the dipole potential at the monolayer collapse ~ 390 mV, is slightly lower than that reported by other authors [20,36]. It is interesting that dipole potential–area dependence for pure gA monolayer (Fig. 2) doesn't exhibit such distinct regions like in the case of DMPC. Incorporation of gA into DMPC monolayer substantially reduced the dipole potential (Fig. 9 B). This agrees well with results reported earlier [20]. In Ref. [20] it was shown that decrease of dipole potential following incorporation of gA couldn't be explained by simple model of coexistence of pure

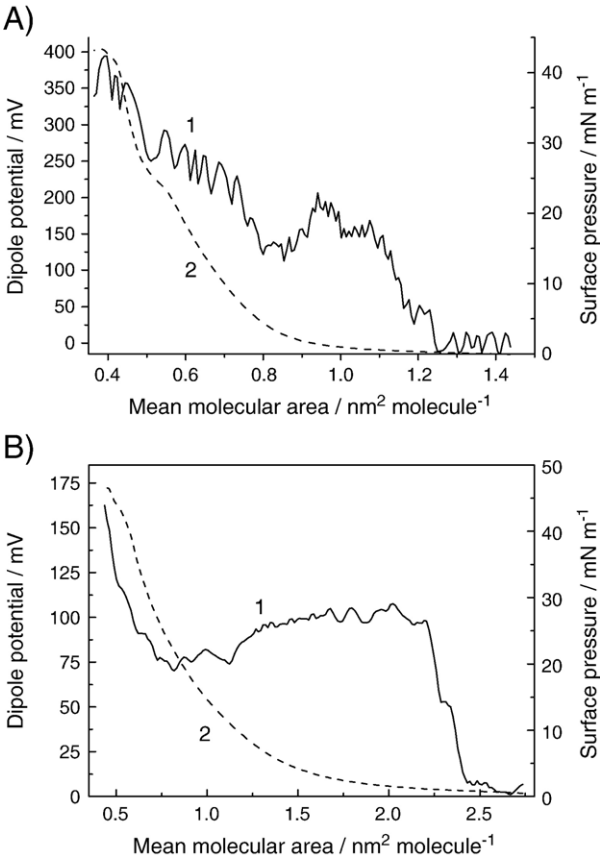

Fig. 9. The plot of 1 — surface potential and 2 — surface pressure as a function of mean molecular area for A) pure DMPC and B) for gA/DMPC mixed monolayer for 0.25 molar fraction of gA. T=18 °C.

lipid and pure gA domains. Certainly, in the case of this simple model, the resulting dipole potential of the mixed monolayer can be calculated according to equation:

$$\Delta V_{12} = X.\Delta V_1 + (1-X).\Delta V_2 \quad (7)$$

where ΔV_1 and ΔV_2 are the dipole potentials for pure components. For example, at π=35 mN/m the dipole potential for pure DMPC monolayer is 323 mV, for pure gA 140 mV and that calculated for mixed monolayer at 0.25 molar fraction of gA is according to Eq. (7) 277 mV. However, the value of dipole potential obtained in our experiment is 130 mV, i.e. only approx. half of the theoretical value. This clearly evidence on strong interaction of gA with lipids.

The shape of the dipole potential–area dependence for mixed gA/DMPC monolayers has certain similarity with that for pure DMPC monolayers. One can see from Fig. 9 A,B that there is no substantial differences in the surface pressure increase for both DMPC and gA/DMPC monolayers in the L-E state of the monolayer. This is most probably due to parallel orientation of the gA main axis in respect of the monolayer surface at L-E state. The main contribution to the surface potential takes place mostly from the changes of tilting of DMPC molecules. When DMPC undergoes transition from L-E to L-C state, the potential decreases. Sharp increase of potential takes place at $\pi \sim 18$ mN/m when the monolayer is in L-C state and gA molecules are tilted. It is likely, that in this case dipole moments of gA and DMPC interacts more strongly. Thus, the interactions between DMPC and gA, as well as between gA molecules contribute to the sharper increase of dipole potential in comparison with pure DMPC monolayer.

3.2.3. MDC of DMPC and of mixed gA/DMPC monolayers

The MDC–area and surface pressure–area plots for DMPC monolayer in a gel state are presented on Fig. 10. The curves correspond to the third compression of the monolayer. Previous two compressions were under the collapse pressure (30 mN/m), while third compression was up to the monolayer collapse. It is seen on the Fig. 10 that similarly like for gA monolayer, there is increase of the current at the beginning of the compression at mean molecular area approx. 1.8 nm^2, when the monolayer is in the gaseous state. The maximum of the peak appears at the area 1.55 nm^2/molecule, exactly when the surface pressure starts to grow. When the compression of monolayer starts, molecules reorient themselves and the projection of the dipole moment of the polar head groups of DMPC increases. Growth of the surface pressure evidences on interaction between lipid molecules that is accompanied by their reorientation as revealed from the changes of MDC. Another maximum of MDC at region 1.2 nm^2/molecule is associated with the plateau at ~ 8 mN/m, where transition of monolayer from L-E to L-C state takes place. In L-C state the monolayer is relatively well ordered and the main contribution to the current comes from the change of the orientation of the molecules. Abrupt increase of the current up to 140 fA at 0.55 nm^2/molecule is typical feature for the orientational ordering in the monolayer in the solid state. This can be connected with orientation of hydrophobic chains of phospholipids [24]. Dramatic decrease of the current at very low area is characteristic for the monolayer collapse.

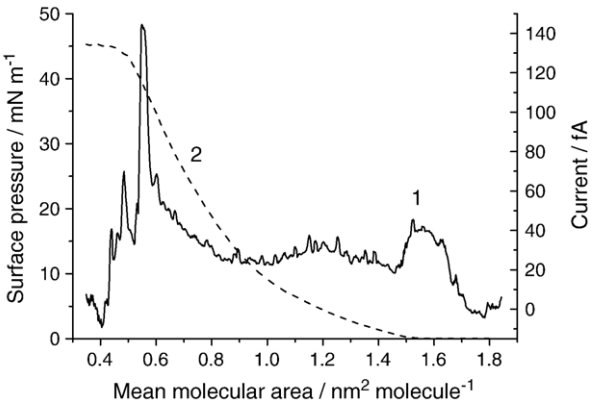

Fig. 10. The plot of Maxwell displacement current (1) and surface pressure (2) versus area of pure DMPC monolayer at T=18 °C. The curves correspond to the third compression of the monolayer. Previous two compressions were under the collapse pressure (30 mN/m), while third compression was up to the monolayer collapse.

MDC–area curves recorded during compression for three different gA/DMPC molar fractions are presented on Fig. 11. All monolayers were compressed three times up to 30 mN/m, followed by expansion of the monolayer. Only plot corresponding to third compression is shown for each molar fraction of gA. We already mentioned that compression below the monolayer collapse is reversible process. In this conditions the MDC–area plot for expansion has shape mirror to that of compression plot (see e.g. Fig. 4). The shape of the MDC–area plot depends on the gA/DMPC molar fraction. One can see on Fig. 11 (curve 1), that for molar fraction of 0.17 gA/DMPC there are two peaks — one at ~ 2 nm^2/molecule and second, broader peak between 0.6 and 1 nm^2/molecule. Two peaks can be found also in the MDC–area curves corresponding to pure DMPC and gA monolayers, respectively. Similar effect was observed for other molar fractions, however with increasing molar fraction of gA, the most remarkable peak (at areas 2, 2.7 and 3.3 nm^2/molecule, respectively) moved in direction of lower area per molecules. It is likely, that resulted MDCs for mixed monolayer represent superposition of the MDCs for pure component and in respect of the peculiarities of the interaction between the gA and lipid molecules. Certain differences in comparison with 0.17 molar fraction take place for 0.25 molar fraction. First a broader maximum with amplitude ~ 30 fA was observed in the liquid-expanded state. Second — deviation at this plot consists in the presence of well-expressed maximum at ~ 1.45 nm^2/molecule. Such a maximum, but considerably weaker and broader, was observed also in the case of pure gA monolayers (Fig. 3). The broad peak at molar fraction 0.25 gA with the maximum at ~ 2.7 nm^2/molecule can be due to accumulation of the molecules under the electrode caused not only by compression of the monolayer, but also due to formation of the gA/DMPC complexes. Certainly, at the molar fraction of 0.25 gA and for DMPC in a gel state (T=18 °C) the complexes of gA/DMPC appear (see Figs. 7 A and 8 A).

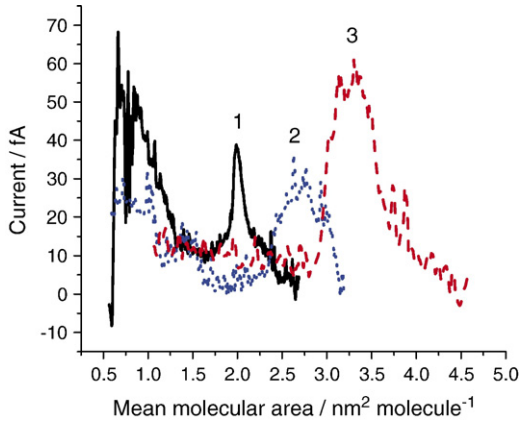

Fig. 11. The plot of current versus area for gA/DMPC at different molar fraction of gA: 1 — 0.17; 2 — 0.25; 3 — 0.5. Each curve corresponds to third compression of the monolayer. All monolayers were compressed up to 30 mN/m. Experiments were performed at $T = 18$ °C.

3.2.4. Dipole moments of the pure DMPC and mixed gA/DMPC monolayers

3.2.4.1. Dipole moment of DMPC monolayers. Pressure and dipole moment–area plots for DMPC monolayers in a gel state for second compression of monolayer are presented on Fig. 12 A. It can be seen that the dipole moment increases up to the region of 1.6 nm^2/molecule, where the surface pressure starts to increase and monolayer slowly undergoes transition from gaseous (G) to L-E state. Small plateau at dipole moment–area plot between 1.45 and 1.6 nm^2/molecule can be probably related to changes of initial reorientation of the molecules at the beginning of the compression. Another increase of the dipole moment projection at 1.45 nm^2/molecule, which rose up to 6.3 a.u. at 0.95 nm^2/molecule, correlates with the condensation process in the L–E state in the monolayer. Please note, that the plot of dipole moment vs. area for DMPC is considerably different from that of gA (Fig. 5). In contrast with gA the dipole moment projection for DMPC continuously increases. This could be due to reorientation and accumulation of the molecules under the electrode. Certainly, DMPC monolayer is characterized by good compressibility at L–E state [36]. Starting at 0.95 nm^2/molecule, monolayer transforms to the L–C state. The L–C and S states are characterized by lower compressibility. In these structural states molecules become closer each to other, but their reorientation is changing only slightly. Therefore dipole moment projection increases not so sharp in comparison with L–E state.

3.2.4.2. Dipole moment of mixed DMPC/gA monolayers. The plots of the dipole moment projections vs. area during compression for three different molar fractions of gA in DMPC monolayers are presented on Fig. 12 B. It can be seen that the shape of the curves depends on the molar fraction of gA in the monolayer. We assume, that the shape of the curves represents superposition of the curves corresponding to the pure components. For molar fraction of 0.17 gA the enhancement of the dipole moment is not so abrupt as in the case of the pure gA (compare with Fig. 5). The maximum of dipole moment of ~ 21 a.u. in the area around 1.7 nm^2/molecule, is probably the result of the primary reorientation of the gA in the monolayer. Due to the presence of the DMPC molecules oriented parallel with the surface or tilted under big angle form the normal to the surface, gA molecules have limited space for reorientation and orient themselves slower. The properties of the monolayer for 0.17 molar fraction of gA and shape of its dipole moment–area curve is in good agreement with the peculiarities of interaction between gA and DMPC molecules, which was discussed above (see Section 3.2.1). Positive deviation from linearity observed on Fig. 7A was attributed to the existence of separate gA and DMPC phases in a monolayer. The presence of two peaks at MDC–area plot (Fig. 11) can be therefore related to the effect of self-orientation of gA and DMPC molecules in a monolayer. Different situation takes place for other molar ratios of gA/DMPC. Similar shape of dipole moment–area curve as in the case of pure gA can be observed at the beginning of the compression up to

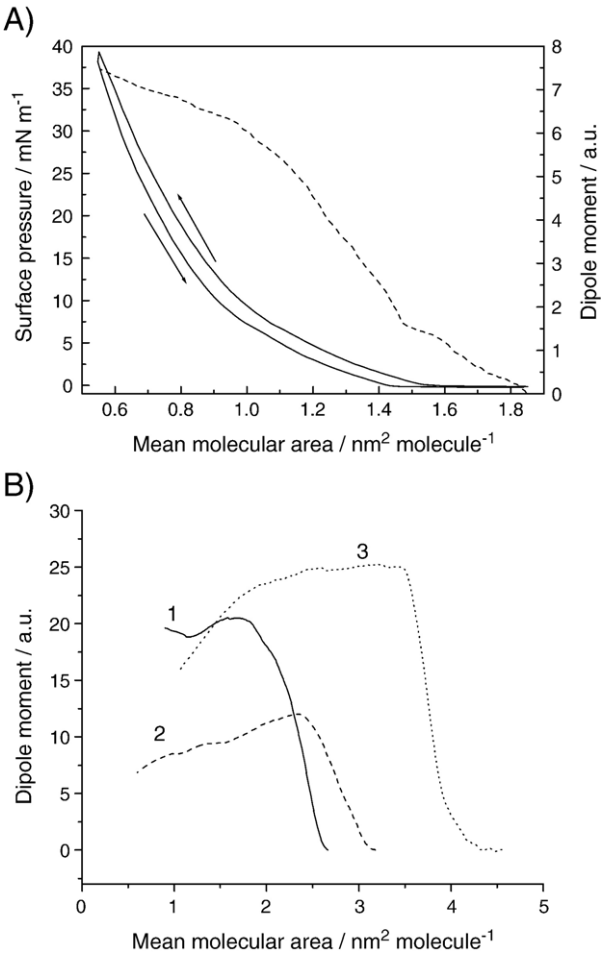

Fig. 12. A) The plot of surface pressure (full line) and dipole moment (dashed line) versus mean molecular area developments of the second compression–expansion cycle of DMPC monolayer. The arrows indicate course of compression and expansion, respectively. B) Dipole moment versus mean molecular area for molar fraction of gA in DMPC monolayers 1 — 0.17; 2 — 0.25 and 3 — 0.5. The curves correspond to the third compressions of the monolayers, which were compressed up to 30 mN/m. The experiments were performed at $T = 18$ °C.

12 a.u. for 0.25 gA/DMPC molar fraction and up to 25 a.u. for 0.5 gA/DMPC molar fraction. The dipole moment projections increase only in the gaseous state of the monolayer. We can speculate, that gA especially at higher molar ratio (0.5) can adopt similar secondary structure like in pure gA monolayers, i.e. double helix. Further compression at 0.5 molar fraction caused only lowering of the dipole moment projection comparing to 0.17 of gA/DMPC molar ratio. Because there is no additional increase of the dipole moment projection, and because even DMPC molecules are still dominant in the monolayer, it can be suggested that interaction between gA and DMPC molecules resulted in formation of the complexes that stabilize monolayer. Further compression of such monolayer does not result in any other substantial changes of orientation of molecules. Study of the surface pressure isotherms for mixed monolayers above 0.17 gA/DMPC molar fraction revealed absence of the plateau corresponding to phase transitions in a monolayer that is typical for pure components and for lower molar fraction of gA/DMPC (i.e. for 0.17 and below) (see Fig. 6A). It was already discussed, that the plateau region (L-E to L-C transition) is characterized by the additional reorientation and accumulation of the molecules. No such effect was observed in the case of 0.25 and 0.5 gA/DMPC molar fractions. We can assume that the ordering of the molecules in the monolayer and favorable interaction caused the formation of a stable monolayer even at lower surface pressure.

4. Conclusion

The method of Maxwell displacement current (MDC) measurement allowed us to observe the structural changes of gA molecules in gA–phospholipid mixture at the air–water interface by the complex analysis of thermodynamic and electric properties. We showed, that these changes, connected probably with formation of secondary structure of gA, take place at rather low mean molecular area in which gA monolayer is in gaseous state. At this state of the monolayers the peak of MDC is observed. Subsequent decrease of the current can be attributed to opposite orientation of dipole moments in a gA due to formation of a double helix. The properties of gA in a mixed monolayer depend on the concentration of the molar fraction of gA in DMPC monolayer. At higher molar fractions of gA/DMPC (around 0.5) the shape of the changes of dipole moment of a mixed monolayer is similar to that of pure gA. This may indicate that double helical conformation of gA could exist or coexist with gA dimers also at the presence of phospholipids.

The study of the pressure–area isotherm for mixed gA/DMPC monolayers in a gel and in a liquid-crystalline state allowed us to show influence of the structural state of the monolayer on the interaction between gA and the phospholipids. In a gel state and at the gA/DMPC molar ratio below 0.17 the aggregates of gA were formed, while above this molar ratio gA interacts favorably with DMPC. In contrast, for DMPC in a liquid-crystalline state aggregation of gA was observed for all molar fractions studied. The effect of formation ordered structures between gA and DMPC as well as aggregation of gA is rather complex and cannot be fully attributed to the mismatch between lipid and peptide hydrophobic side.

Acknowledgements

This work was supported by NATO Collaborative linkage grant (LST.CLG.978567 to T.H.), by the Agency for Promotion Research and Development under the contract No. APVT-51-013904, VEGA (Projects No. 1/1015/04 to T.H. and 1/3038/06 to J.C.), Ministry of Education of Slovak Republic and Comenius University grant for young researchers (to P.V.).

References

[1] J.A. Killian, Gramicidin and gramicidin–lipid interactions, Biochim. Biophys. Acta 1113 (1992) 391–452.
[2] B.A. Wallace, Recent advances in high-resolution structures of bacterial channels: gramicidin A, J. Struct. Biol. 121 (1998) 123–141.
[3] R. Sarges, B. Witkop, The structure of valine- and isoleucine-gramicidin A, J. Am. Chem. Soc. 87 (1965) 2011–2020.
[4] D.W. Urry, The gramicidin A transmembrane channel: a proposed $\pi_{(L,D)}$ helix, PNAS 68 (1971) 672–676.
[5] R.R. Ketchem, W. Hu, T.A. Cross, High-resolution conformation of gramicidin A in a lipid bilayer by solid-state NMR, Science 261 (1993) 1457–1460.
[6] O.S. Andersen, H.J. Appel, E. Bamberg, D.D. Busath, Gramicidin channel controversy — the structure in lipid environment, Nat. Struct. Biol. 6 (1999) 609.
[7] R.R. Ketchem, B. Roux, T.A. Cross, Computational refinement through solid state NMR and energy constraints of a membrane bound polypeptide, in: K. Mertz Jr., B. Roux (Eds.), Biological Membranes, Birkhauser Press, 1996, pp. 299–322.
[8] T.B. Woolf, B. Roux, Structure, energetics, and dynamics of lipid–protein interactions: a molecular dynamics study of the gramicidin A channel in DMPC bilayer, Proteins 24 (1996) 92–114.
[9] G. Kim, M.C. Gurau, S.M. Lim, P.S. Cremer, Investigations of orientation of membrane peptide by sum frequency spectroscopy, J. Phys. Chem., B 107 (2003) 1403–1409.
[10] O.S. Andersen, Kinetics of ion movement mediated by carriers and channels, Methods Enzymol. 171 (1989) 62–112.
[11] T.B. Woolf, B. Roux, Molecular dynamics simulation of the gramicidin channel in a phospholipid bilayer, Proc. Natl. Acad. Sci. U. S. A. 91 (1994) 11631–11635.
[12] S.W. Chiu, S. Subramaniam, E. Jakobsson, Simulation studies of a gramicidin/lipid bilayer system in excess water and lipid. 1. Structure of the molecular system, Biophys. J. 76 (1999) 1929–1938.
[13] H. Lavoie, D. Blaudez, D. Vaknin, B. Desbat, B.M. Ocko, Ch. Salesse, Spectroscopic and structural properties of valine gramicidin A in monolayer at water–air interface, Biophys. J. 83 (2002) 1–12.
[14] W.-P. Ulrich, H. Vogel, Polarization-modulated FTIR spectroscopy of lipid/gramicidin monolayers at the air/water interface, Biophys. J. 76 (1999) 1639–1647.
[15] M. Diociaiuti, F. Bordi, A. Motta, A. Carosi, A. Molinari, G. Arancia, C. Coluzza, Aggregation of gramicidin A in phospholipid Langmuir monolayers, Biophys. J. 82 (2002) 3198–3206.
[16] J. Mou, D.M. Czajkowski, Z. Shao, Gramicidin A aggregation in supported gel state phosphatidylcholine bilayers, Biochemistry 35 (1996) 3222–3226.
[17] M.D. Becker, D.V. Greathouse, R.E. Koeppe, O.S. Andersen, Amino acid sequence modulation of gramicidin channel function: effect of tryptophan-to-phenylalanine substitution on the single-channel conductance and duration, Biochemistry 30 (1991) 8830–8839.
[18] D.D. Busath, C.D. Thulin, R.W. Hendershot, L.R. Phillips, P. Maughan, C.D. Cole, N.C Bingham, S. Morrison, L.C. Baird, R.J. Hendershot, M. Cotten, T.A Cross, Noncontact dipole effect on channel permeation. 1. Experiments with (5F-indole) Trp^{13} gramicidin A channels, Biophys. J. 75 (1998) 2830–2844.
[19] V. Vogel, D. Möbius, Local surface potentials and electric dipole moments of lipid monolayers: contributions of the water/lipid and the lipid/air interfaces, J. Colloid Interface Sci. 126 (1988) 408–422.

[20] V.L. Shapovalov, E.A. Kotova, T.I. Rokitskaya, Y.N. Antonenko, Effect of gramicidin A on the dipole potential of phospholipid membranes, Biophys. J. 77 (1999) 299–305.
[21] P. Dynarowicz-Łątka, Modern physicochemical research on Langmuir monolayers, Adv. Colloid Interface Sci. 91 (2001) 221–293.
[22] M. Iwamoto, Y. Majima, Investigations of the dynamic behavior of fatty acid monolayers at the air–water interface using a displacement current-measuring technique coupled with the Langmuir-film technique, J. Chem. Phys. 94 (1991) 5135–5142.
[23] H. Brockman, Dipole potential of lipid membranes, Chem. Phys. Lipids 73 (1994) 57–79.
[24] J. Cirák, P. Tomčík, D. Barančok, A. Bolognesi, M. Ragazzi, Dipole moment of a modified poly(3-alkylthiophene) at air/water interface, Thin Solid Films 402 (2002) 190–194.
[25] G. Kemp, C. Werner, Solution, interfacial, and membrane properties of gramicidin A, Arch. Biochem. Biophys. 176 (1976) 547–555.
[26] N.D. Mau, P. Daumas, D. Lelievre, Y. Trudelle, F. Heitz, Linear gramicidins at the air–water interface, Biophys. J. 51 (1987) 843–845.
[27] H. Tournois, P. Gieles, R. Demel, J. de Gier, B. de Kruijff, Interfacial properties of gramicidin and gramicidin–lipid mixtures measured with static and dynamic monolayer techniques, Biophys. J. 55 (1989) 557–569.
[28] D. Ducharme, D. Vaknin, M. Paudler, C. Salesse, H. Riegler, H. Möhwald, Surface properties of valine–gramicidin A at the air/water interface, Thin Solid Films 284–285 (1996) 90–93.
[29] S. Vitovič, R. Kresák, R. Naumann, S.M. Schiller, R.N.A.H. Lewis, R.N. McElhaney, T. Hianik, The study of the interaction of a model α-helical peptide with lipid bilayers and monolayers, Bioelectrochemistry 63 (2004) 169–176.
[30] G.L. Gaines Jr., Insoluble Monolayers at Liquid–Gas Interface, John Wiley and Sons, New York, 1966.
[31] M.C. Phillips, D. Chapman, Monolayer characteristics of saturated 1,2-diacylphosphatidyl-cholines (lecithins) and phosphatidylethanolamines at the air–water interface, Biochim. Biophys. Acta. 163 (1968) 301–313.
[32] R. Maget-Dana, The monolayer technique: a potential tool for studying the interfacial properties of antimicrobial and membrane-lytic peptides and their interactions with lipid membranes, Biochim. Biophys. Acta. 1462 (1999) 109–140.
[33] D. Marsh, Lateral pressure in membranes, Biochim. Biophys. Acta. 1286 (1996) 186–223.
[34] Y.-P. Zhang, R.N.A.H. Lewis, R.S. Hodges, R.N. McElhaney, Interaction of α-helical segment of a membrane protein with phosphatidylcholine bilayers: differential scanning calorimetry and FTIR spectroscopic studies, Biochemistry 31 (1992) 11579–11588.
[35] B.A. Cornell, F. Separovic, A model for gramicidin A-phospholipid interactions in bilayers, Eur. Biophys. J. 15 (1988) 299–306.
[36] J.M. Holopainen, H.L. Brockman, R.E. Brown, P.K.J. Kinnunen, Interfacial interactions of ceramide with dimyristoylphosphatidylcholine: impact of the *N*-acyl chain, Biophys. J. 80 (2001) 765–775.